Redox tuning of cytochrome b562 through facile metal porphyrin substitution

ARTICLE *in* CHEMICAL COMMUNICATIONS · SEPTEMBER 2012

Impact Factor: 6.83 · DOI: 10.1039/c2cc34302a · Source: PubMed

6 AUTHORS, INCLUDING:

Qijin Chi
Technical University of Denmark
98 PUBLICATIONS **2,293** CITATIONS
SEE PROFILE

Martin - Elliott
Cardiff University
85 PUBLICATIONS **1,006** CITATIONS
SEE PROFILE

Emyr Macdonald
Cardiff University
33 PUBLICATIONS **650** CITATIONS
SEE PROFILE

D. Dafydd Jones
Cardiff University
43 PUBLICATIONS **543** CITATIONS
SEE PROFILE

ChemComm

Cite this: *Chem. Commun.*, 2012, **48**, 10624–10626

www.rsc.org/chemcomm

COMMUNICATION

Redox tuning of cytochrome b_{562} through facile metal porphyrin substitution†

Eduardo Antonio Della Pia,[ac] Qijin Chi,*[b] Martin Elliott,[c] J. Emyr Macdonald,[c] Jens Ulstrup[b] and D. Dafydd Jones*[a]

Received 15th June 2012, Accepted 7th September 2012
DOI: 10.1039/c2cc34302a

The biologically and nanotechnologically important heme protein cytochrome b_{562} was reconstructed with zinc and copper porphyrins, leading to significant changes in the spectral, redox and electron transfer properties. The Cu form shifts the redox potential by +300 mV and exhibits high electron transfer, while the Zn form is redox inert.

Metalloproteins comprise one of the most abundant protein groups in nature; between a third to half of all natural proteins bind metal ions.[1] This class of proteins is of particular importance as they are involved in a variety of key biological processes[2] and, over the past decade, significant progress has been made for their integration in hybrid bio-electronic devices.[3] The metal ion plays a key role defining the activity of a protein either indirectly through determining the conformation or directly through involvement in the mechanism of function. A variety of different metal ions are utilised in nature, among which the most important ones are Zn^{2+}, $Fe^{2+/3+}$ and $Cu^{+/2+}$. Zn^{2+} is an important structural metal but also contributes to activating water for hydrolysis reactions.[4] Both Fe and Cu are largely involved in electron transfer processes.[5,6] Fe in the form of heme (iron protoporphyrin IX) is particularly important as it plays central roles in photosynthesis, respiration, transport and catalysis. Natural heme proteins show a wide range of redox potentials (650 mV) tuned mainly by interactions with the protein scaffold and the axial ligands.[5] As well as being involved in electron transfer pathways in photosynthetic chains, several Cu-containing proteins facilitate electron flow between electron donors and dioxygen.[6]

The ability of individual metalloprotein molecules to self-assemble and modulate the properties of the bound metal ion make them attractive for use as active single molecule nanoscale components and materials. Furthermore, the move from bulk to single molecule metalloprotein approaches and analysis will ultimately lead to new fundamental functional and mechanistic insights. Simple, robust redox active proteins are particularly attractive as single molecule devices as they exhibit transistor-like behaviour.[7] Gating is achieved *via* electrochemical and biochemical events that alter the redox potential which in turns modulates electron transfer or current flow characteristics. One such protein that could be considered ideal for such applications is cytochrome b_{562} (cyt b_{562}). Cyt b_{562} is a small redox-active protein found in *E. coli* that has a four helical bundle structure that coordinates to the heme iron through the axial ligands Methionine 7 (Met7) and Histidine 102 (His102) (Fig. 1(a)).[8] Cyt b_{562} has proved particularly useful for the fundamental understanding of the electron transfer process in proteins and for the development of new bioelectronics devices.[7] It can also be linked to other proteins so the functional centres are coupled.[9]

Crucially, we have recently shown that cyt b_{562} can be designed to bind non-biological surfaces such as gold in defined orientations through the introduction of a cysteine amino acid at specific points in the protein structure.[7] The introduction of a thiol group

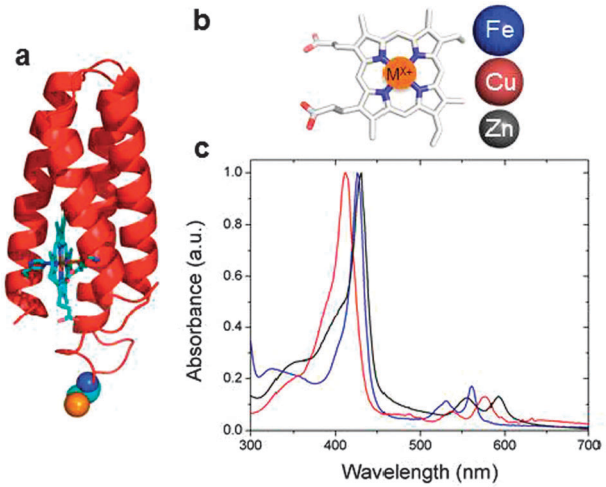

Fig. 1 (a) Structure of holo-cyt b_{562} (PDB, 256B). The cyt b_{562} ribbon structure is coloured red, the heme group is shown in light blue and the amino acid targeted for mutation is highlighted as spheres. (b) Chemical structure of (blue) iron, (red) copper and (black) zinc protoporphyrin IX. (c) Normalized UV-Vis spectra of 20 μM D50C cyt b_{562} reconstructed with (blue) 20 μM heme, (red) 20 μM Cu-PP and (black) 20 μM Zn-PP in 10 mM phosphate buffer pH 6.2.

[a] *School of Biosciences, Main Building, Cardiff University, Cardiff CF10 3AT, UK. E-mail: jonesdd@cardiff.ac.uk*
[b] *Department of Chemistry and NanoDTU, Technical University of Denmark, DK-2800 Lyngby, Denmark. E-mail: cq@kemi.dtu.dk*
[c] *School of Physics and Astronomy, Queens' Building, Cardiff University, Cardiff CF24 3AA, UK*

† Electronic supplementary information (ESI) available: Materials and methods, SDS-PAGE analysis, spectrophotometric titration of D50C apo-cyt b_{562} with Zn-PP and Cu-PP, UV-Vis and Far UV circular dichroism spectra of Zn-PP and Cu-PP cyt b_{562}, cyclic voltammetry of the Cu-PP, Laviron's plot. See DOI: 10.1039/c2cc34302a

by exchanging an aspartate for cysteine at residue 50 (D50C) has proved particularly useful.[7] Using engineered proteins in conjunction with single molecule STM studies has allowed us to demonstrate that cyt b_{562} is highly conductive with conductance being electrochemically gated.[10] The ability to tune the redox potentials and add different conducting centres would thus expand the application of cyt b_{562} and improve our fundamental understanding of metal–protein interactions. There has been some success in varying the redox potential of cyt b_{562} through conventional protein mutagenesis by tuning the protein's interactions with the heme group.[5,11] However, this approach has generally resulted in lowering the redox potential and has been restricted to sampling the Fe^{2+}/Fe^{3+} centre.[5,11] Also, as these engineered proteins do not bind directly to metallic electrodes, direct electron transfer cannot be realised or is relatively slow.

In the present study we combine two approaches to measure and modulate the redox properties of cyt b_{562}; utilisation of the D50C variant to facilitate defined and direct binding to a single gold electrode,[7] which in turn allows direct investigation of the effect of metal ion replacement through facile co-factor exchange. As *b*-type cytochromes bind heme non-covalently *via* axial ligands, heme can be easily removed and replaced by other porphyrins with the metal centre substituted with redox active copper protoporphyrin IX (Cu-PP) and photoactivatable zinc protoporphyrin IX (Zn-PP) (Fig. 1(b)). The use of the cyt b_{562} D50C variant will allow cyclic voltammetric methods based on well defined atomically planar single-crystal electrodes to be used.

Cyt b_{562} was generated to high purity and homogeneity (Fig. S1, ESI†). Binding of Zn-PP and Cu-PP to cyt b_{562} D50C monitored by UV-Vis spectroscopy resulted in markedly different spectral characteristics compared to the heme bound form (Fig. 1(c)). A significant red shift (~36 nm) and a narrower bandwidth were observed for both the Zn-PP and Cu-PP Soret Band on addition to apo-cyt b_{562}, which can be interpreted as incorporation of the PPs into the protein (Fig. S2 and S3, ESI†). Far UV circular dichroism (CD) spectroscopy further indicates that Cu-PP and Zn-PP bind in a similar fashion to heme (Fig. S4, ESI†). Apo-cyt b_{562} is only partially folded and heme binding within the active pocket of the protein results in a structural transition towards stable formation of the helical bundle structure (Fig. 1(a)).[8] The increase in helical signatures (troughs at 208 and 222 nm) in the CD spectra of cyt b_{562} D50C associated with heme binding are observed in the presence of either Cu-PP or Zn-PP. The virtually identical CD spectra of cyt b_{562} reconstituted with heme, Cu-PP or Zn-PP further support that the protein scaffold and co-factor binding mode remains intact on metal substitution.

The Soret band in all holo-protein forms was observed together with the α and β bands (Fig. 1(c)). Cyt b_{562}-Zn-PP has peaks at 431 nm (Soret band), 558 nm (β-band) and 592 nm (α-band) and a broad shoulder at 360 nm. The spectra of the D50C cyt b_{562} reconstructed with Cu-PP shows peaks at 414 nm (Soret band), 537 nm (β-band) and 579 nm (α-band) and a shoulder at 350 nm. The holo-cyt b_{562} (with heme bound) shows an intense Soret band at 427 nm.[9,12] Changes in the axial ligand coordination of the cyt b_{562}'s Met7 and His102 amino acids to the Zn-PP and Cu-PP might account for the shift of the Soret band towards higher (Zn-PP) and lower (Cu-PP) wavelengths in comparison to the heme-cyt b_{562}. In particular the Soret peak of the cyt b_{562}-Cu-PP at 414 nm suggests a 5-coordinated Cu-PP complex[13] and the ratio $\varepsilon_\alpha/\varepsilon_\beta > 1$ is evidence of coordination of the Cu-PP to a nitrogen acceptor.[14]

An established spectroscopic approach[15] was used to measure the affinity of cyt b_{562} (K_d) for each of the PPs by measuring the increase in Soret band absorbance on addition of PP. Both the Cu-PP and Zn-PP titrations indicated that approximately one molecule of apo-protein binds with one PP molecule (Fig. S5 and S6, ESI†). The K_d values of Zn-PP and Cu-PP for cyt b_{562} were 500 ± 80 nM and 100 ± 30 nM, respectively. These values are at least one order of magnitude higher than the K_d values calculated for the oxidised heme-apo-cyt b_{562} complex,[9,12] indicating that the affinity for Cu-PP and Zn-PP is lower but still relatively high in biological terms.

The redox properties of high purity cyt b_{562} reconstructed with the redox inactive Zn-PP or redox active Cu-PP (Fig. S1, ESI†) were investigated by cyclic voltammetry. Holo-protein was adsorbed in a defined manner onto the Au(111) surface *via* the thiol group introduced at residue 50.[7] The Cu-PP cyt b_{562} displayed stable and reversible electrochemical characteristics in keeping with cycling between the Cu^+ and Cu^{2+} states. Direct electron transfer was consistently detected by normal cyclic voltammetry, indicating effective electronic coupling between the Cu-PP center and the electrode. Fig. 2(a) shows an example of the reversible cyclic voltammogram recorded for this system. A pair of well-defined redox peaks was observed with a formal redox potential ($E^{0\prime}$) of 205 ± 5 mV *vs.* SCE. Cathodic and anodic peaks are not completely symmetric, suggesting that the protein does not retain its original conformation or surface orientation upon copper oxidation, or more likely that the coordination of the Cu-PP with the protein's active site changes upon its oxidation. It is noticeable that the redox potential is significantly different from that for the Cu-PP alone measured in homogeneous solution state (50 ± 2 mV *vs.* SCE; Fig. S7, ESI†). This observation is a clear indication that despite not being the cytochrome's native cofactor, the polypeptide scaffold plays a crucial role in the redox chemistry of Cu-PP making it a much stronger oxidising agent and might be viewed as a facilitator of electron transfer between the redox center and the electrode. The substitution of the central metal has also a major effect on the redox potential of the cyt b_{562}, shifting it positively by *ca.* 300 mV compared to heme-cyt b_{562}. This difference could be rooted in the axial binding of the electronically "soft" His102 (and perhaps Met7) ligand(s) favouring the low oxidation of copper.[8] This change is significantly

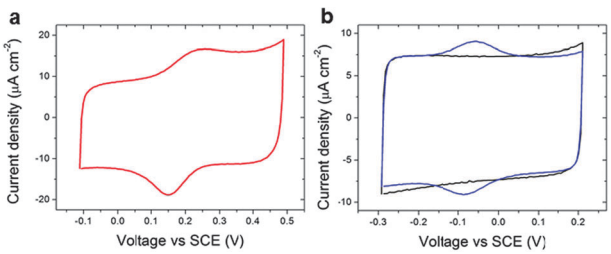

Fig. 2 Cyclic voltammogram of cyt b_{562} D50C reconstructed with (a) Cu-PP (red line) and (b) heme (blue line) or (b) Zn-PP (black line). Protein samples were self-assembled on Au(111) in 10 mM phosphate buffer pH 6.2. Scan rate is 1 V s^{-1}.

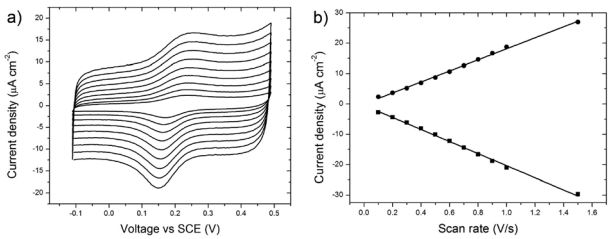

Fig. 3 (a) Cyclic voltammograms at various scan rates (from 0.1 V s^{-1} to 1 V s^{-1}) of cyt b_{562} D50C reconstructed with Cu-PP and deposited on Au(111) in 10 mM phosphate buffer pH 6.2. (b) Corresponding relation between the anodic (circle dots) and cathodic (square dots) peak currents and scan rates. The solid lines are the best linear fits of the experimental data.

larger than has been achieved solely through protein mutagenesis[16] and shifts the reduction potential to a higher rather than lower value with respect to the heme-bound cyt b_{562} form.[11]

The cathodic and anodic peak currents obtained from cyclic voltammograms depend linearly on the scan rate up to 1.5 V s^{-1} (Fig. 3(a)) suggesting that the electron transfer process is controlled by the surface process (*i.e.* diffusionless system) and that the proteins are strongly adsorbed onto the electrode. The surface coverage calculated from the slope of the linear fitting of the peak current density against scan rate data ($(11.4 \pm 0.8) \times 10^{12}$ molecules per cm^2) indicates an almost full monolayer coverage of the Au(111) surface with electroactive proteins.

The electron transfer rate constant was evaluated from the observed redox peak current separation variation with the sweep rates in the range 12–22 V s^{-1} according to Laviron's method (Fig. S8, ESI†).[17] The rate of electron transfer (14 ± 2 s^{-1}) obtained is close to the one determined for the heme-cyt b_{562} (44 s^{-1}).[8] Thus, the substitution of Cu-PP enhances the oxidizing ability of the cyt b_{562}, but retains ET efficiency despite apparent changes in axial ligand coordination. The small difference in ET rate between the Cu-PP and the heme substituted cyt b_{562} could be ascribed to the different polarization of the redox binding pocket that affects the reorganization energy of the proteins, the dominating parameter controlling the ET rate.

No redox activity was measured for the Zn PP-cyt b_{562} (Fig. 2(b)) demonstrating that the presence of the redox metal centre (Fe or Cu) is crucial in the protein's electron transfer characteristics. The capacitive background current of the heme-cyt b_{562} is very similar to the one of Zn-PP cyt b_{562} system indicating that the protein's hydrophobic residues are not exposed to the supporting electrolyte. This result, in conjunction with the measured UV-Vis and CD spectra (Fig. 1(c)), supports that the cytochrome maintains its folded tertiary structure when reconstructed with the Zn-PP.

We have shown that the metal centre engineering achieved by protoporphyrin IX replacement can alter the electronic properties of cyt b_{562}. Cyt b_{562} is thus a good acceptor and modulator of different metal centre protoporphyrins thus potentially expanding its capacity to sample a range of metal centres and properties. While Zn-PP renders cyt b_{562} electrochemically inert, changing the iron center to copper shifts the redox potential positively by 300 mV, while preserving the native holo-protein structure and its electron transfer properties. This change is higher than that currently achieved through traditional protein engineering. The protein itself shifts the redox potential of Cu-PP by 150 mV. It is also likely that replacing Fe with Cu goes beyond simply changing the redox potential but also the electron transfer mechanism. Engineering the metal centre therefore provides a new route to altering and tuning the redox and electron transfer characteristics of metalloproteins such as cyt b_{562}.

This work was supported by the BBSRC (Grant BB/E001084 to D.D.J.) and EPSRC (Grant EP/D076072/1 to J.E.M. and M.E.) in UK and by the Lundbeck Foundation (to Q.C.) and Danish Research Council for Technology and Production Sciences (Contract No. 274-07-0272 to Q.C. and J.U.) in Denmark. E.A.D.P. acknowledges the Cardiff University Richard Whipp Interdisciplinary Research Scholarship for PhD study.

Notes and references

1 C. L. Dupont, A. Butcher, R. E. Valas, P. E. Bourne and G. Caetano-Anollés, *Proc. Natl. Acad. Sci. U. S. A.*, 2010, **107**, 10567–10572.
2 C. R. Robinson, Y. Liu, J. A. Thomson, J. M. Sturtevant and S. G. Sligar, *Biochemistry*, 1997, **36**, 16141–16146.
3 J. Zhang, Q. Chi, A. M. Kuznetsov, A. G. Hansen, H. Wackerbarth, H. E. M. Christensen, J. E. T. Andersen and J. Ulstrup, *J. Phys. Chem. B*, 2002, **106**, 1131–1152; J. Zhang, A. M. Kuznetsov, I. G. Medvedev, Q. Chi, T. Albrecht, P. S. Jensen and J. Ulstrup, *Chem. Rev.*, 2008, **108**, 2737–2791.
4 J. E. Coleman, *Curr. Opin. Chem. Biol.*, 1998, **2**, 222–234.
5 C. J. Reedy, M. M. Elvekrog and B. R. Gibney, *Nucleic Acids Res.*, 2008, **36**, 307A–313A; D. S. Wuttke and H. B. Gray, *Curr. Opin. Struct. Biol.*, 1993, **3**, 555–563.
6 H. B. Gray, B. G. Malmström and R. J. Williams, *J. Biol. Inorg. Chem.*, 2000, **5**, 551–559; R. K. Szilagyi and E. I. Solomon, *Curr. Opin. Chem. Biol.*, 2002, **6**, 250–258.
7 E. A. Della Pia, Q. Chi, D. D. Jones, J. E. Macdonald, J. Ulstrup and M. Elliott, *Nano Lett.*, 2011, **11**, 176–182; E. A. Della Pia, M. Elliott, D. D. Jones and J. E. Macdonald, *ACS Nano*, 2012, **6**, 355–361.
8 Y. Feng, S. G. Sligar and A. J. Wand, *Nat. Struct. Biol.*, 1994, **1**, 30–35; D. W. Low, M. G. Hill, M. R. Carrasco, S. B. H. Kent and P. Botti, *Proc. Natl. Acad. Sci. U. S. A.*, 2001, **98**, 6554–6559.
9 D. D. Jones and P. D. Barker, *Angew. Chem., Int. Ed.*, 2005, **44**, 6337–6341; D. D. Jones and P. D. Barker, *ChemBioChem*, 2004, **5**, 964–971; J. A. J. Arpino, H. Czapinska, A. Piasecka, W. R. Edwards, P. Barker, M. J. Gajda, M. Bochtler and D. D. Jones, *J. Am. Chem. Soc.*, 2012, **134**, 13632–13640.
10 E. A. Della Pia, Q. Chi, J. E. Macdonald, J. Ulstrup, D. D. Jones and M. Elliott, *Nanoscale*, accepted.
11 Y. Mie, F. Mizutani, T. Uno, C. Yamada, K. Nishiyama and I. Taniguchi, *J. Inorg. Biochem.*, 2005, **99**, 1245–1249; S. L. Springs, S. E. Bass and G. L. McLendon, *Biochemistry*, 2000, **39**, 6075–6082; S. L. Springs, S. E. Bass, G. Bowman, I. Nodelman, C. E. Schutt and G. L. McLendon, *Biochemistry*, 2002, **41**, 4321–4328.
12 E. Itagaki, G. Palmer and L. P. Hager, *J. Biol. Chem.*, 1967, **242**, 2272–2277.
13 B. Venkatesha, H. Horia, G. Miyazakia, S. Nagatomob, T. Kitagawab and H. Morimoto, *J. Inorg. Biochem.*, 2002, **88**, 310–315; P. T. Manoharan, K. Alston and J. M. Rifkind, *J. Am. Chem. Soc.*, 1986, **108**, 7095–7100; K. Alston and C. B. Storm, *Biochemistry*, 1979, **18**, 4292–4300.
14 R. E. Sharp, J. R. Diers, D. F. Bocian and P. L. Dutton, *J. Am. Chem. Soc.*, 1998, **120**, 7103–7104; H. Anni, J. M. Vanderkooi and L. Mayne, *Biochemistry*, 1995, **34**, 5744–5753.
15 Z. X. Wang, N. R. Kumar and D. K. Srivastava, *Anal. Biochem.*, 1992, **206**, 376–381.
16 K. Hamada, P. H. Bethge and F. S. Mathews, *J. Mol. Biol.*, 1995, **247**, 947–962; P. D. Barker, J. L. Butler, P. De Oliveira, H. A. O. Hill and N. I. Hunt, *Inorg. Chim. Acta*, 1996, **252**, 71–77; S. L. Springs, S. E. Bass and G. L. McLendon, *Biochemistry*, 2000, **39**, 6075–6082.
17 E. Laviron, *J. Electroanal. Chem.*, 1979, **101**, 19–28.

Chemical Communications

SUPPLEMENTARY INFORMATION

Redox tuning of cytochrome b_{562} through facile metal porphyrin substitution

Eduardo Antonio Della Pia,[a, b] Qijin Chi,[c] Martin Elliott,[b] J. Emyr Macdonald,[b] Jens Ulstrup,[c] D. Dafydd Jones, *[a]

Materials and Methods

Sample preparation. Construction of the Asp50 to Cys mutant (D50C) of cyt b_{562} has been described previously.[1] Apo-cyt b_{562} D50C was extracted from the periplasmic fraction of *E. coli* and purified as outlined previously.[1]

Copper protoporphyrin IX (Cu-PP) and zinc protoporphyrin IX (Zn-PP) were purchased from Santa Cruz biotechnology, Inc. US. The molecules were dissolved in 1 M NaOH prior to use. To avoid molecular aggregation and photodegradation, Zn-PP and Cu-PP solutions were stored in the dark, kept at 4 °C and centrifuged prior experiments. To reconstitute holo-cyt b_{562} with different metalloporphyrins, excess of protoporphyrin (~ 10 molar equivalents) was added to apo-cyt b_{562} D50C in 10 mM phosphate buffer pH 6.2. The mixture was then incubated in the dark at 4 °C overnight and purified using centrifugal filters (3kDa cut-off). The purity of the resulting samples was verified through SDS-PAGE analysis (Figure S1). Only a single band was observed that corresponds to the molecular weight of cyt b_{562} D50C (12 kDa).[2]

Absorption and circular dichroism spectroscopy. UV-Vis absorption spectra were measured on a Hewlett-Packard (HP) 8450A diode array UV-Vis spectrophotometer at 25°C. Apo-cyt b_{562} D50C concentration was determined by measuring the absorbance at 280 nm (extinction coefficient 3.0 mM^{-1} cm^{-1}).[2] Cu-PP and Zn-PP affinity for cyt b_{562} D50C were performed as described previously.[1] CD spectroscopy was performed in 1.0 cm path length quartz cuvettes on a Jasco J-710 spectropolarimeter. Spectra were collected from 190 to 250 nm with a response time of 1 s and an increment of 0.2 nm. The reported spectra are the average of 5 scans. Base lines obtained from samples containing only buffer were subtracted from all the data reported.

Electrochemical measurements. Au(111) electrodes were electrochemically etched in 1 M H_2SO_4 and washed with 1 M HCl and water, then annealed for 8 hours at 880 °C.[3, 4] Prior to protein deposition the electrodes were annealed with a H_2 flame and the Au(111) single crystal surface was protected with hydrogen saturated water. The electrodes were subsequently incubated in 50-60 µM protein solution at 4 °C overnight. Prior to undertaking the experiments the electrodes were rinsed with water to remove the non-chemically adsorbed molecules. The proteins were checked for stability by measuring the UV-Vis spectra before and after the incubation. Electrochemical measurements were performed using an Autolab potentiostat (Eco Chemie, Netherlands) controlled by a general purpose electrochemical software package (GPES). Cyclic voltammetry experiments were carried out in a single-compartment glass cell consisting of a gold working electrode, a platinum wire gaze auxiliary electrode, and a freshly realized reversible hydrogen reference electrode (RHE). The RHE potential was measured against SCE potential at the end of each experiment and the obtained values used to correct the measured potentials. A constant gas stream of purified Argon was flowed through the electrochemical cell prior and during the experiments to generate an inert atmosphere. The sample was allowed to equilibrate for 5 minutes in the same buffer as the protein, 10 mM phosphate buffer pH 6.2.

Results

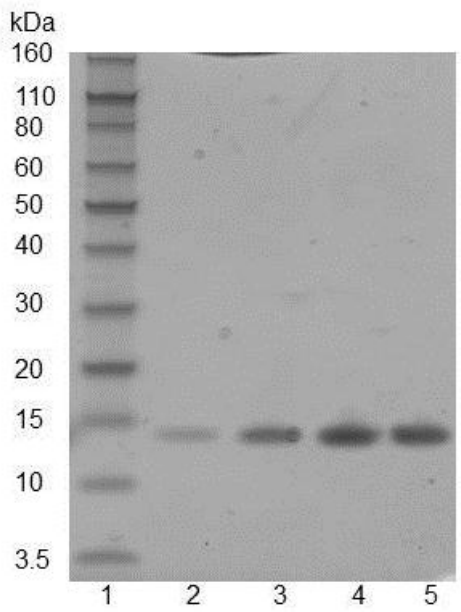

Figure S1. SDS-PAGE analysis of D50C cyt b_{562}. Lane 1, protein molecular weight standards; lane 2 apo-cyt b_{562} D50C; lane 3 D50C cyt b_{562} reconstructed with heme; lane 4 D50C cyt b_{562} reconstructed with Cu-PP; lane 4 D50C cyt b_{562} reconstructed with Zn-PP.

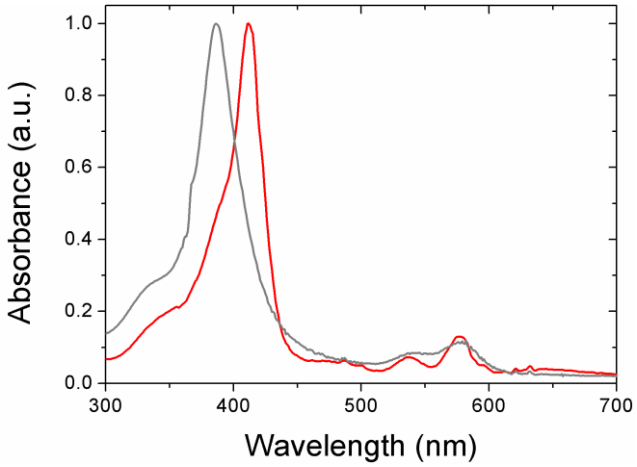

Figure S2. Normalized UV-Vis spectrum of 20 μM of Cu-PP alone (grey line) or 20 μM cyt b_{562} D50C reconstructed with 20 μM Cu-PP (red line). All spectra were recorded in 10 mM phosphate buffer pH 6.2.

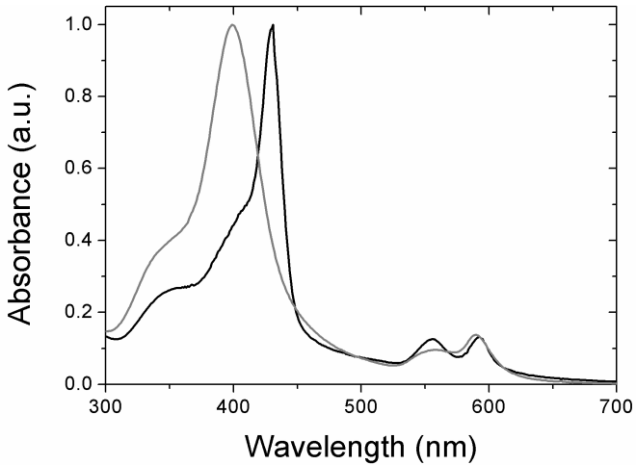

Figure S3. Normalized UV-Vis spectrum of either 20 μM of Zn-PP alone or 20 μM cyt b_{562} D50C reconstructed with 20 μM Zn-PP (black line) (grey line). All spectra were recorded in 10 mM phosphate buffer pH 6.2.

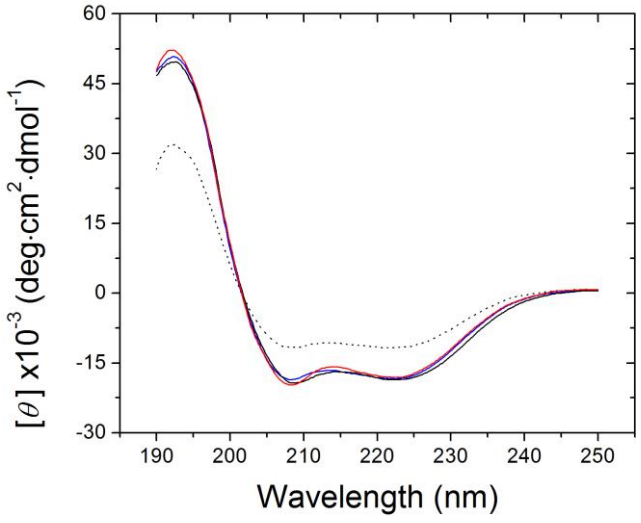

Figure S4. Far UV circular dichroism spectra of apo-cyt b_{562} D50C (dotted line), cyt b_{562} D50C reconstructed with heme (blue), Cu-PP (red) and Zn-PP (black) in 10 mM phosphate buffer pH 6.2 at 25°C. The proteins concentrations were 10 μM.

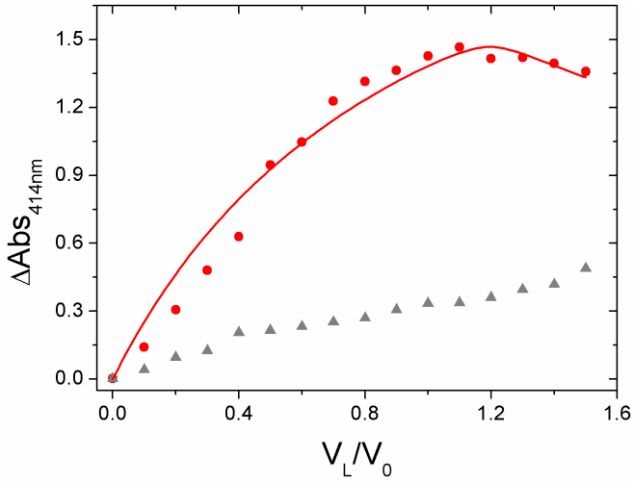

Figure S5. Spectrophotometric titration of apo-cyt b_{562} D50C with Cu-PP (red). Aliquots of Cu-PP sampling a final concentration range of 0 to 15 μM were titrated into 1 ml of 20 μM apo-cyt b_{562} D50C in 10 mM phosphate buffer pH 6.2. A blank (grey) titration of Cu-PP into buffer is also shown (grey). Error bars are not shown to improve the clarity of the figure.

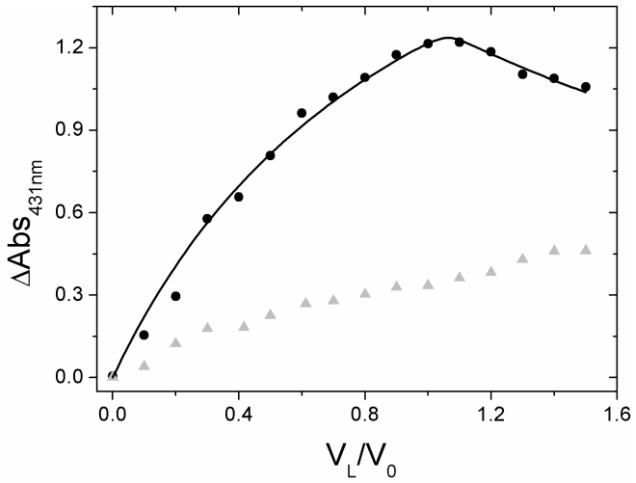

Figure S6. Spectrophotometric titration of apo-cyt b_{562} D50C with Zn-PP (red). Aliquots of Zn-PP sampling a final concentration range of 0 to 15 μM were titrated into 1 ml of 20 μM apo-cyt b_{562} D50C in 10 mM phosphate buffer pH 6.2. A blank (grey) titration of Cu-PP into buffer is also shown (grey). Error bars are not shown to improve the clarity of the figure.

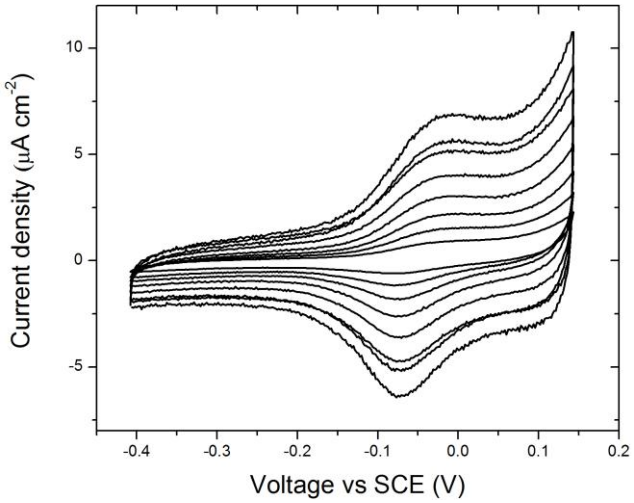

Figure S7. Cyclic voltammetry of Cu-PP in 10 mM phosphate buffer pH 6.2 at various scan rates (from 0.1 Vs^{-1} to 0.9 Vs^{-1}). For performing the experiment 1 ml of 100 µM Cu-PP in 0.1 M NaOH were dissolved in 5 ml of 10 mM phosphate buffer pH 6.2.

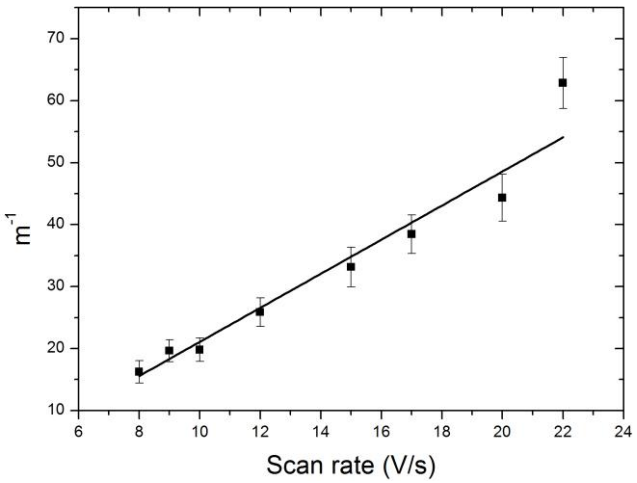

Figure S8. Plot of m^{-1} versus scan rate. The m values were obtained from the peak separations in the cyclic voltammograms. The solid curve is the best linear fit of the experimental data

Notes and references

[a] *School of Biosciences, Main Building, Cardiff University, Cardiff CF10 3AT, UK; E-mail: jonesdd@cardiff.ac.uk.*
[b] *School of Physics and Astronomy, Queens' Building, Cardiff University, Cardiff CF24 3AA, UK.*
[c] *Department of Chemistry and NanoDTU, Technical University of Denmark, DK-2800 Lyngby, Denmark.*

[1] E. A. Della Pia, Q. Chi, D. D. Jones, J. E. Macdonald, J. Ulstrup and M. Elliott, *Nano Lett.*, 2011, **11**, 176-182.
[2] Y. Feng, S. G. Sligar and A. J. Wand, *Nat. Struct. Biol.*, 1994, **1**, 30–35.
[3] A. Hamelin and A.M. Martins, *J. Electroanal. Chem.*, 1996, **407**, 13-21.
[4] J. Clavilier, R. Faure, G. Guinet, R. Durand, *J. Electroanal. Chem.*, 1979, **1**, 198- 205.